Critical Dynamics of Cross-Linked Polymer Chains near the Gelation Threshold

Masanao Takeda, Tomohisa Norisuye, and Mitsuhiro Shibayama*

Department of Polymer Science and Engineering, Kyoto Institute of Technology, Matsugasaki, Sakyo-ku, Kyoto 606-8585, Japan

Received December 15, 1999; Revised Manuscript Received February 21, 2000

ABSTRACT: The dynamics of cross-linked polymer chains in solution near the gelation threshold has been investigated by dynamic light scattering. The time−intensity correlation function (ICF) was obtained as a function of initial monomer concentration, C_{NIPA}, and cross-linker concentration, C_{BIS}, where NIPA and BIS denote *N*-isopropylacrylamide and *N*,*N*′-methylenebis(acrylamide), respectively. The ICF exhibited a distinct change at a unique set of (C_{NIPA}, C_{BIS}) for a given R_{BIS} ($\equiv 2C_{BIS}/(C_{NIPA} + 2C_{BIS})$), i.e., (1) from a stretched exponential to a clear power-law behavior and (2) depression of the initial amplitude of ICF. According to the previous work [Norisuye et al. *Macromolecules* **1998**, *31*, 5316], this point was determined to be the gelation threshold, (C_{NIPA}^{th}, C_{BIS}^{th}). The locus of (C_{NIPA}^{th}, C_{BIS}^{th}) was a decreasing function of C_{NIPA}^{th} with the lower cutoff at $C_{NIPA}^{th} \approx C_{NIPA}^*$ and was in good agreement with the prediction of the site-bond percolation theory, where C_{NIPA}^* is the so-called chain overlap concentration. Several characteristic features at this connectivity transition point, such as anomaly in the scattered intensity and the power-law exponent, are discussed as critical dynamics.

Introduction

Polymer chain dynamics has been extensively investigated by dynamic light scattering (DLS) in dilute, semidilute, and concentrated solutions.[1] Compared to the dynamics of linear polymers and ion-containing polymers, that of cross-linked polymers has been less investigated, particularly that near gelation threshold. One of the characteristic features of the gelation threshold is that the time−intensity correlation function (ICF), $g^{(2)}(\tau)$, exhibits a characteristic behavior with a power-law fashion, i.e., $g^{(2)}(\tau) - 1 \sim \tau^{n-1}$, exclusively at the gelation threshold, where *n* is the power-law exponent and $0 < n < 1$.[2] The appearance of a power-law behavior at gelation threshold has been often observed during gelation process by many investigators, e.g., Martin et al. (tetramethoxysilane gel),[3,4] Lang and Burchard (polysaccharide gel),[5] and Ren et al. (gelatin gel).[6] Adam and Lairez extensively discussed the power law behavior for the chain dynamics at the sol−gel transition of polymer gels in connection with percolation theory.[7]

In the previous paper,[8] dynamic light scattering (DLS) studies were conducted on the chain dynamics of cross-linked poly(*N*-isopropylacrylamide) (NIPA) as a function of monomer concentrations, C_{NIPA}, where the cross-linker (*N*,*N*′-methylenebis(acrylamide); BIS) concentration, C_{BIS}, was fixed to 8.62 mM. The results were compared with those of linear polymer chains. A power-law behavior similar to those reported in the literature was observed in the ICF exclusively in the cross-linked systems around $C_{NIPA} \approx 100$ mM as shown with the solid lines in Figure 1, while such a power-law behavior was not observed for linear polymer chains at all. The solid line in the figure is the fit with a power-law function (see eq 7). However, unlike the case of the gelation process studied by Martin et al. and others, the fit was not satisfactorily enough to conclude that a power-law behavior is an indication of the gelation threshold. This was mainly due to the fact that the set of monomer and cross-linker concentrations, (C_{NIPA}, C_{BIS}), was not close enough to match the condition for the gelation threshold. Further experiments on NIPA gels as well as other gels, such as silica gels,[9] clearly showed an appearance of power-law behavior. Hence, we believe now that the power-law behavior is one of the characteristic features of the gelation threshold. In other words, a power-law behavior in ICF is an indication of the connectivity transition of network chains.

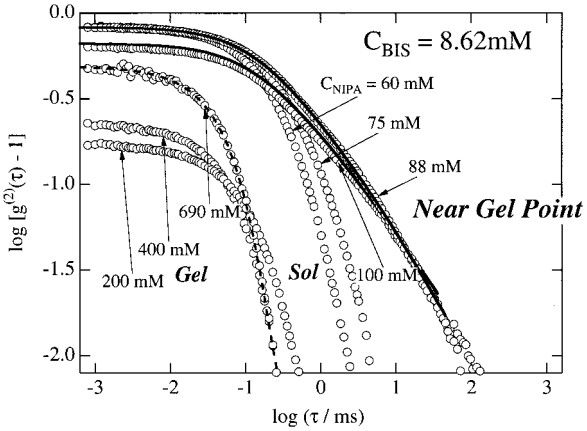

Figure 1. Double-logarithmic plot of the intensity−time correlation function (ICF), $g^{(2)}(\tau) - 1$, for cross-linked NIPA polymer chains in a solvent with various C_{NIPA}'s. The solid and dashed lines indicate the fits with a power-law function and an single-exponential function, respectively.

Another interesting feature in Figure 1 is that the ICF for the cross-linked system with $C_{NIPA} \gg 100$ mM is reduced to a single-exponential behavior as shown by the dashed lines (see eq 1). This was predicted and verified experimentally as collective diffusion by Tanaka et al.[10] Even today, however, no consensus on the functional form of ICF for gels after the gelation threshold has been obtained, since some gels, such as siloxane gels[4] and poly(vinyl alcohol) gels,[11] do not exhibit a single-exponential behavior at all. In any case, the appearance of a power-law behavior at the gelation

* To whom correspondence should be addressed.

10.1021/ma9921044 CCC: $19.00
Published on Web 03/31/2000

threshold is significant, which indicates the connectivity divergence at the gelation threshold.

In this paper, we dig into this problem more deeply by varying both C_{NIPA} and C_{BIS}. A sol−gel phase diagram will be constructed as a function of C_{NIPA} and C_{BIS} and will be compared with the prediction by site-bond percolation theory.[12] Then, the characteristic features of the critical dynamics will be addressed.

Theoretical Background

According to the collective diffusion theory for polymer gels,[10] the intensity−time correlation function (ICF), $g^{(2)}(\tau)$, for polymer networks in a solvent can be given by a single-exponential function, as follows:

$$g^{(2)}(\tau) - 1 = \sigma_I^2 \exp[-2\Gamma\tau] \quad (1)$$

where τ is the decay time, σ_I^2 is the initial amplitude of the correlation function, and Γ is the characteristic decay rate for the collective diffusion of the network in the gel. Γ is related to the collective diffusion coefficient, D, with the following equation:

$$\Gamma = Dq^2 \quad (2)$$

where q is the scattering vector. Two important facts should be noted here. First, eq 1 is valid only for monodisperse ergodic media, such as for monodisperse latex solutions and linear polymer solutions in the dilute and semidilute regime. In the case of polymer gels (nonergodic media), the scattering element is allowed only a limited excursion with a finite spatial extent.[13] Hence, $g^{(2)}(\tau)$ becomes sample position dependent and has both homodyne and heterodyne components dependent on the sample position, p, as is written by[14]

$$g_p^{(2)}(\tau) - 1 = X_p^2\{g^{(1)}(\tau)\}^2 + 2X_p(1 - X_p)g^{(1)}(\tau) \cong \sigma_{I,p}^2 \exp[-2\Gamma_{A,p}\tau] \quad \text{(for small } \tau) \quad (3)$$

where $\Gamma_{A,p}$ is the apparent characteristic decay time. Here, $g^{(1)}(\tau) \equiv \exp(-\Gamma\tau)$ is the scattering field correlation function, X_p is the ratio of the intensities of the fluctuating component $\langle I_F\rangle_T$ to the total intensity $\langle I\rangle_{T,p}$, i.e., $X_p \equiv \langle I_F\rangle_T/\langle I\rangle_{T,p}$, and $\langle ...\rangle_T$ denotes time average. Here, the subscript p indicates the variable is sample position dependent. Hence, the initial amplitude of ICF, $\sigma_{I,p}^2$

$$\sigma_{I,p}^2 \equiv g_p^{(2)}(0) - 1 = X_p(2 - X_p) \quad (4)$$

is significantly reduced from unity due to nonergodicity ($0 < X_p \ll 1$). To describe such nonergodic media, one needs to take an ensemble average of the correlation function over many sample positions, p. The ensemble average intensity, $g_E^{(2)}(\tau)$, and the field correlation functions, $g_E^{(1)}(\tau)$, are defined by

$$g_E^{(2)}(\tau) \equiv \frac{\sum_p \langle I(0)\, I(\tau)\rangle_{T,p}}{\sum_p \langle I(0)\rangle_{T,p}^2} = \frac{\sum_p \langle I(0)\rangle_{T,p}^2 g_p^{(2)}(\tau)}{\sum_p \langle I(0)\rangle_{T,p}^2} \quad (5)$$

$$g_E^{(1)}(\tau) \equiv \sqrt{g_E^{(2)}(\tau) - 1} \quad (6)$$

The characteristic feature of nonergodicity is $g_E^{(1)}(\tau \to \infty) \neq 0$.

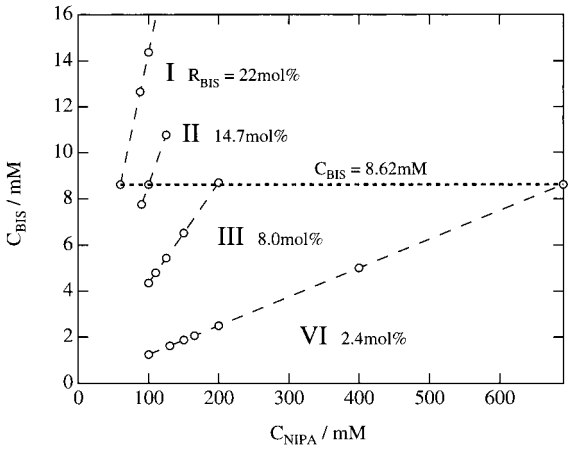

Figure 2. Mapping of the initial monomer and cross-linker concentrations, (C_{NIPA}, C_{BIS}). The dashed and dotted line indicate the case with iso-R_{BIS} and iso-C_{BIS}, respectively.

Second, the functional form of ICF becomes a non-exponential function at the gelation threshold because of the presence of polymer chain clusters with different sizes. Particularly, at the gelation threshold, infinite networks with an assembly of self-similar clusters having finite sizes appear and become dominant, exhibiting a power-law behavior in ICF in the wide range of τ. Since the collective diffusion mode is preserved for small τ's, the ICF is written in the following form:[4]

$$g^{(2)}(\tau) - 1 = \left\{A \exp(-\Gamma\tau) + (1 - A)\left(1 + \frac{\tau}{\tau^*}\right)^{(n-1)/2}\right\}^2 \quad (7)$$

where A is the amplitude of the collective diffusion mode, τ^* is the lower cutoff of the power-law behavior, and n is the power-law exponent. Note that n is the same as the viscoelastic exponent appearing in the angular frequency (ω) dependence in the storage, $G'(\omega)$ and shear moduli, $G''(\omega)$, i.e.,[7,15,16]

$$G'(\omega) = G''(\omega) \sim \omega^n \quad (8)$$

The value of n is dependent on the degree of branching of the polymer and the degrees of screening of the excluded-volume effect as well as the hydrodynamic interaction.[17,18]

Experimental Section

Samples. A series of cross-linked poly(*N*-isopropylacrylamide) (NIPA) were prepared by redox polymerization in aqueous media. The monomer concentration of NIPA at preparation, C_{NIPA}, and the cross-linker concentration (*N*,*N*′-methylenebisacrylamide; BIS) C_{BIS}, were varied by keeping the ratio R_{BIS} ($\equiv 2C_{BIS}/(C_{NIPA} + 2C_{BIS})$) to be 2.4, 8.0, 14.7, and 22 mol % as shown with the dashed lines in Figure 2. The dotted line, on the other hand, indicates the monomer and cross-linker concentrations employed in the previous paper, the case of fixed C_{BIS} (=8.62 mM).[8] The initiator concentration (ammonium persulfate) was fixed to be 1.75 mM. These monomers and reagents were dissolved in distilled water, filtered with a 0.2 μm filter, and then degassed. After chilling the mixture solutions in a refrigerator for about 30 min, polymerization was initiated in a 10 mm glass test tube at 20 °C by adding 8 mM tetramethylethylenediamine (catalyst).

Dynamic Light Scattering. Dynamic light scattering (DLS) measurements were carried out on cross-linked poly-NIPA aqueous systems with a DLS/SLS-5000 compact goniometer, ALV, Langen, coupled with an ALV photon correlator. A 22 mW helium−neon laser (the wavelength in a vacuum; λ

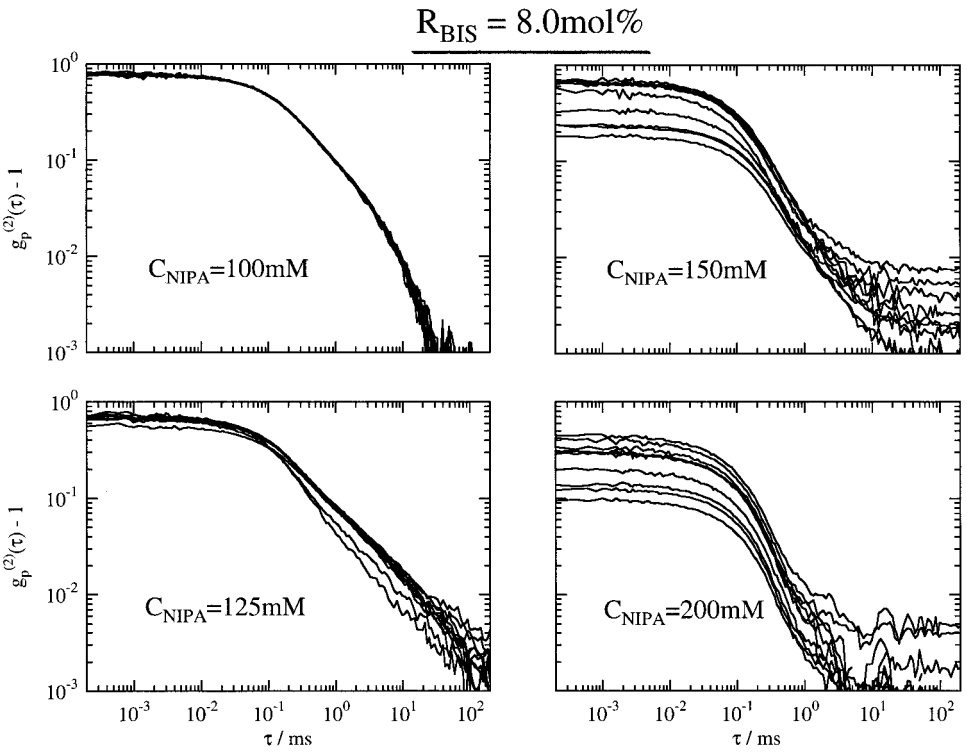

Figure 3. Series of ICFs, $g_p^{(2)}(\tau) - 1$, for cross-linked poly-NIPA with $R_{BIS} = 8.0$ mol %. The subscript p denotes that the variable depends on the sample position. The NIPA monomer concentrations were varied from 100 to 125, 150, and 200 mM, according to Figure 2.

= 632.8 nm) was used as the incident beam. All the measurements were carried out at 20 °C at the scattering angle of 90°. The acquisition time for each run was 30 s.

Results and Discussion

Determination of the Gelation Threshold and Construction of Phase Diagram. Figure 3 shows double-logarithmic plots of the ICFs, $\log[g_p^{(2)}(\tau) - 1]$, for cross-linked NIPA polymer chains with $C_{NIPA} = 100$, 125, 150, and 200 mM. The monomer/cross-link concentration ratio, R_{BIS} was fixed to be 8.0 mol %. For each C_{NIPA}, 10 of ICFs were obtained at different sample positions in order to examine the nonergodicity of the system. For $C_{NIPA} = 100$ mM, all of ICFs collapse to a single curve, indicating that the system is ergodic. At $C_{NIPA} = 125$ mM, a power-law behavior is clearly observed for $10^{-1} \le \tau \le 10^2$ ms. By further increasing C_{NIPA} (=150 and 200 mM), the ICFs deviate from a power law behavior at $\tau > 10^0$ ms and become sample position dependent, e.g., scattering in the initial amplitude of ICF. Therefore, it is clear that $C_{NIPA} \approx 125$ mM is the gelation threshold for $R_{BIS} = 8.0$ mol %.

Similar analyses were carried out for different R_{BIS}'s. Figure 4 shows typical ICFs for NIPA gels with $R_{BIS} =$ 22.3 (I), 14.7 (II), 8.0 (III), and 2.4 mol % (IV). The solid lines are the fits with eq 7. The gelation threshold was evaluated to be $C_{NIPA}{}^{th} \approx 100$ mM (I), 100 mM (II), 125 mM (III), and 165 mM (IV). It should be noted here that in the case of low R_{BIS}, e.g., $R_{BIS} = 2.4$ mol %, a clear crossover from a collective diffusion mode to a power-law mode is observed as indicated by the arrow in IV.

Figure 5 shows the sol−gel phase diagram of NIPA−BIS copolymers in aqueous solutions. Both open and filled circles denote the concentrations (C_{NIPA}, C_{BIS}) at which DLS measurements were conducted. The solid squares indicate that the system was opaque (phase separated; two phase), and circles denote the system was transparent (one phase). The filled circles indicate the concentration ($C_{NIPA}{}^{th}$, $C_{BIS}{}^{th}$) at which a power law behavior in ICF was observed. Hence, the locus of the filled circles, represented with the thick solid line, indicates the sol−gel phase boundary. This sol−gel phase diagram reminds one of the prediction of the site-bond percolation theory.[12] Three interesting features can be drawn from this figure. First, $C_{BIS}{}^{th}$ is a decreasing function of $C_{NIPA}{}^{th}$. Second, there exists the lower bound of $C_{NIPA}{}^{th}$ below which no gelation takes place. We verified that $C_{NIPA}{}^{th}$ is nearly equal to the so-called chain overlap concentration, $C_{NIPA}{}^*$, of the corresponding poly-NIPA solution.[8,19,20] Third, the presence of the binodal line (shown with the thin solid line) was also experimentally observed. All of the three features are in accord with the prediction of the percolation theory. We believe that this is the first time to reproduce the sol−gel phase diagram as well as the coexistence curve at least by scattering measurements.

Collective Diffusion Mode vs Cluster Mode. In Figure 4, it was conjectured that the shape of ICF depends on R_{BIS} at the gelation threshold (e.g., the solid lines in Figure 4). To understand this more quantitatively, we plotted the value of A (the fraction of the collective diffusion mode) as a function of R_{BIS} in Figure 6. Interestingly, A is a monotonic decreasing function of R_{BIS}. For $R_{BIS} \ge 14.7$ mol %, the ICF does not show any clear crossover from the collective to cluster mode (see II of Figure 4). Here, the collective and cluster modes mean a single-exponential behavior and a power-law behavior, respectively. However, reduction of R_{BIS} results in a decoupling of the two modes as demonstrated in III and IV of Figure 4. This means that the collective diffusion mode is well preserved for a slightly cross-linked gel (such as the case of $R_{BIS} = 2.4$ mol %). Typical gels, e.g., polyacrylamide gels for electrophoresis, are formed with $R_{BIS} \approx 2.4$ mol %. This is why those

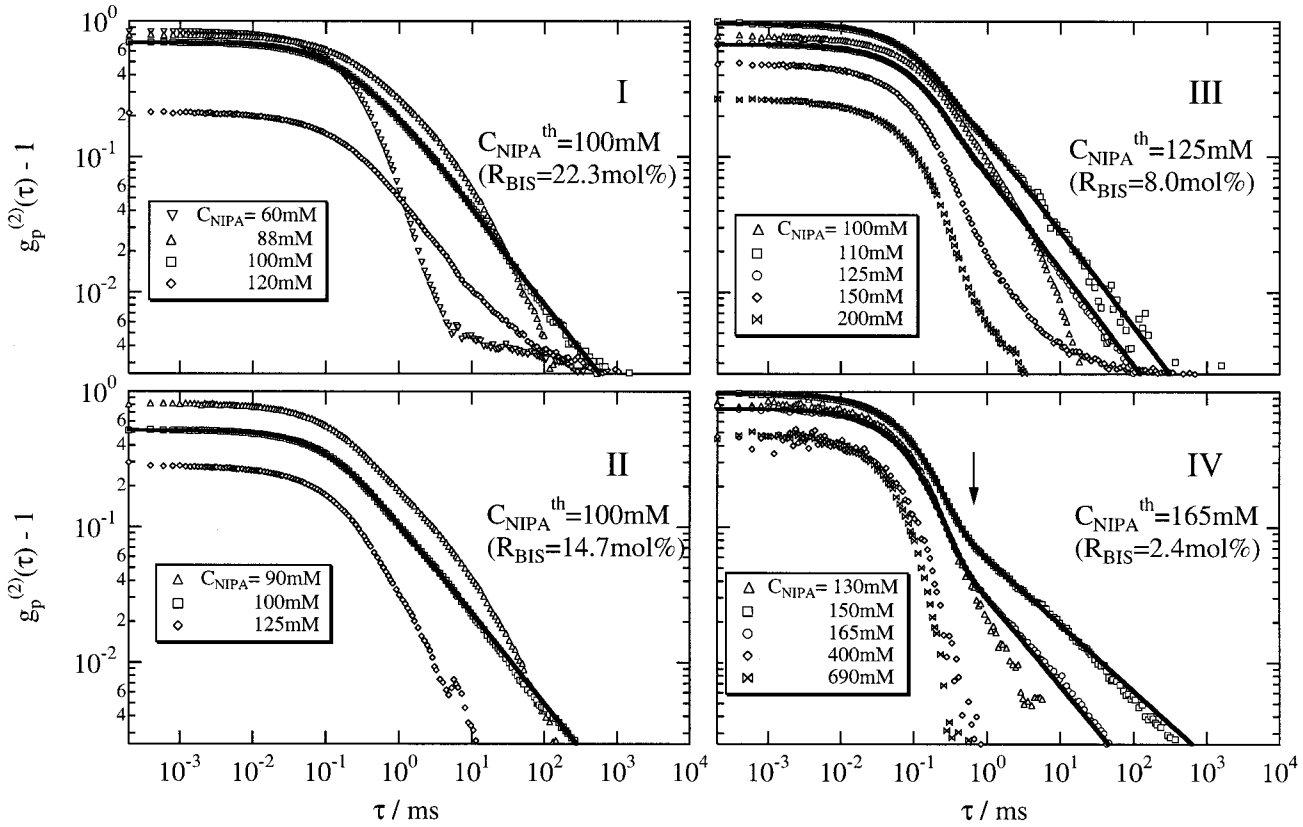

Figure 4. Series of ICFs for cross-linked poly-NIPA with various R_{BIS}'s. The NIPA concentration at gelation, i.e., C_{NIPA}^{th}, is indicated in the figure.

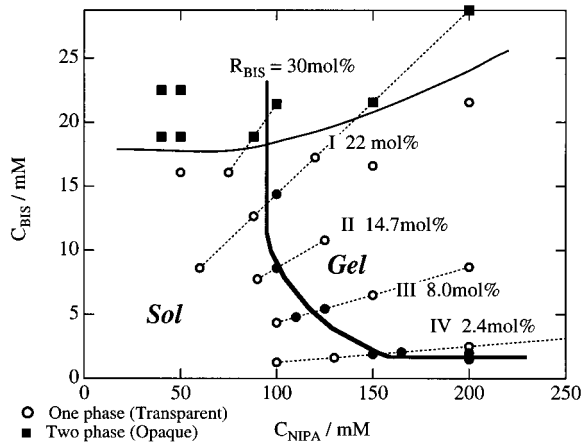

Figure 5. Phase diagram of poly-NIPA/BIS cross-linked system. The solid circles indicate that the (C_{NIPA}, C_{BIS}) concentrations at which the ICF became a power-law function. The thick solid line indicates the sol−gel transition obtained by DLS; the thin solid line represent the binodal line above which the system became opaque (solid squares). The dashed line is tied for samples with the same R_{BIS}.

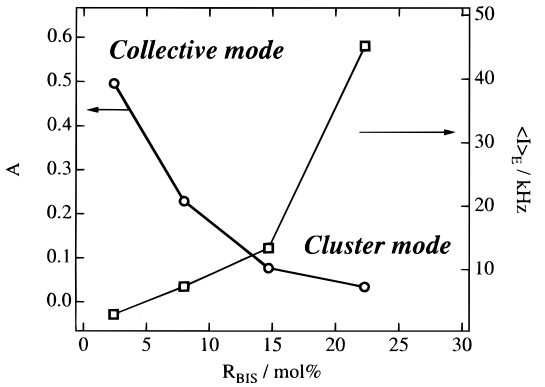

Figure 6. R_{BIS} dependence of the fraction of the collective diffusion mode, A, and the ensemble average scattered intensity, $\langle I\rangle_E$.

gels have been analyzed only in the context of collective diffusion mode.[10] On the other hand, the suppression of the collective mode and domination of a power-law behavior for larger R_{BIS}'s may suggest that the degree of connectivity inhomogeneities increases and polymer chain clusters become more exclusive at the gelation threshold with increasing cross-link density, R_{BIS}.

In Figure 6 is also plotted the ensemble average scattered intensity, $\langle I\rangle_E$, as a function of R_{BIS}. $\langle I\rangle_E$ was obtained by taking ensemble average of $\langle I\rangle_T$, measured at 100 different sample positions. The details of the method to obtain $\langle I\rangle_E$ are described elsewhere.[21] Since $\langle I\rangle_E$ is a measure of the static inhomogeneities, the increase in $\langle I\rangle_E$ indicates that both concentration and connectivity inhomogeneities increase with increasing R_{BIS}. Accordingly, the contribution of the collective diffusion mode A decreases with R_{BIS}.

The Power-Law Exponent. As discussed in the theoretical section, the critical exponent, n, has the same physical origin as the power-law behavior[16,22] in the viscoelastic behavior at the gelation threshold (see eq 8). By taking account of hydrodynamic screening effects, Muthukumar[23] and Martin et al.[24] derived the relation between n and the fractal dimension d_f,

$$n = \frac{d}{d_f + 2} \tag{9}$$

where d is the space dimension (=3). By substituting

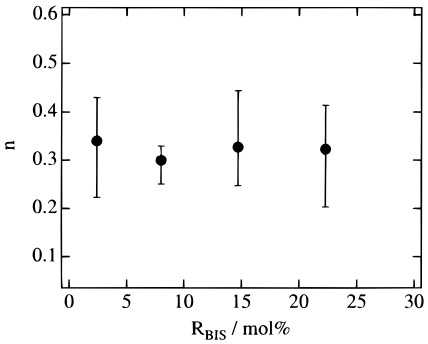

Figure 7. R_{BIS} dependence of the power-law exponent, n. The error bar indicates the largest and smallest values of n, and solid circle is their average.

$d_f = 2$, n is readily obtained to be $^3/_4$. In the case of percolated clusters, $d_f = 2.52$ leads to $n = {}^2/_3$. In the case when the excluded-volume effect is screened, d_f should be replaced by $\overline{d}_f = 2d_f/(d + 2 - 2d_f)$ as discussed by Muthukumar,[17,23] i.e.,

$$n = \frac{d}{\overline{d}_f + 2} = \frac{d(d + 2 - 2d_f)}{2(d + 2 - d_f)} \tag{10}$$

This is the case of this study where a reactor batch gel without dilution is considered. Hence, n becomes to $^1/_2$ when $d_f = 2$. According to the theory, the value of n can be even smaller than $^1/_2$ if d_f approaches the value of the percolation clusters, i.e., $d_f = 2.52$. Antonietti et al. observed a variation of the n value from 0.2 to 0.5 for end-linked polystyrene networks having different degrees of polymerization between cross-links by viscoelasticity measurements.[25]

Figure 7 shows the R_{BIS} dependence of n. The error bar indicates the largest and lowest values of n obtained at 100 different sample positions. Such a large variation of n for a given R_{BIS} is due to the fact that each DLS measurement provides information only on the local scattering volume of the order of 0.1 mm^3, and the information is highly sample position dependent in the case of nonergodic media. The filled circles indicate arithmetic average of the value of n. The degree of branching was expected to increase with R_{BIS}, which should have resulted in an increase in d_f. According to eq 10, n is a decreasing function of d_f (hence a decreasing function of R_{BIS}, too). However, the observed values of n are around 0.3 irrespective of R_{BIS}. This unexpected result may be accounted for as follows. Figure 5 indicates that the higher the R_{BIS}, the lower the $C_{NIPA}{}^{th}$ is. Therefore, the decrease in n with increasing R_{BIS} is canceled by an increase in n with decreasing $C_{NIPA}{}^{th}$. This hypothesis needs to be examined by further experiments.

Decomposition of the Scattered Intensity and Nonergodicity Effects for Postgelation Gels. In one of our previous papers,[19] we reported that the scattered intensity is highest at the gelation threshold, i.e., the sol−gel transition, for a series of gels with a fixed C_{BIS}. This phenomenon is analogous to critical opalescence appearing at a gas−liquid transition of low-molecular-weight fluids. We decomposed the scattered intensity $\langle I\rangle_{T,p}$ to those from thermal fluctuations, $\langle I_F\rangle_T$, and from static inhomogeneities, $\langle I_C\rangle_{T,p} \equiv \langle I\rangle_{T,p} - \langle I_F\rangle_T$, according to the method described elsewhere.[21] However, this method can only be applied to gels far above the gelation threshold but not to gels near the threshold. Joosten proposed, on the other hand, a decomposition method by using ensemble average scattered intensity.[14] According to this method, the ratio of $\langle I_F\rangle_T$ and $\langle I\rangle_E$ can be obtained as follows:

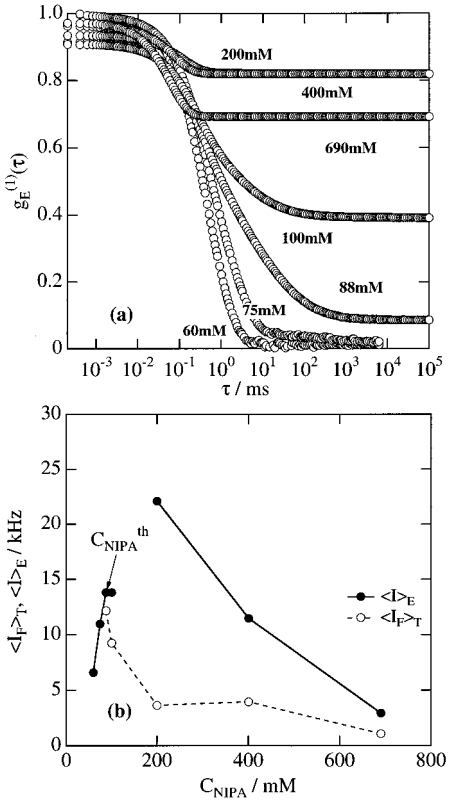

Figure 8. (a) Variation of the scattering field correlation function, $g_E^{(1)}(\tau)$, with C_{NIPA}. (b) C_{NIPA} dependence of the scattered intensity component from thermal fluctuations, $\langle I_F\rangle_T$, and $\langle I\rangle_E$ for NIPA gels with fixed C_{NIPA} (=8.62 mM).

$$\frac{\langle I_F\rangle_T}{\langle I\rangle_E} = 1 - g_E^{(1)}(\tau \to \infty) \tag{11}$$

Figure 8a shows the ensemble average scattering field correlation function, $g_E^{(1)}(\tau)$. The nonergodicity, indicated by none zero value of $g_E^{(1)}(\infty)$, already appears at $C_{NIPA} = 88$ mM and reaches its maximum around $C_{NIPA} \approx 200$ mM. Figure 8b shows $\langle I\rangle_E$ and $\langle I_F\rangle_T$ for NIPA gels prepared with fixed C_{BIS} (=8.62 mM). The NIPA concentration at gelation threshold is indicated with $C_{NIPA}{}^{th}$. It is needless to mention that $\langle I\rangle_E = \langle I_F\rangle_T$ for $C_{NIPA} \le C_{NIPA}{}^{th}$. For $C_{NIPA} > C_{NIPA}{}^{th}$, $\langle I\rangle_E$ is much larger than $\langle I_F\rangle_T$, and both $\langle I\rangle_E$ and $\langle I_F\rangle_T$ are decreasing function of C_{NIPA}. The decrease in $\langle I\rangle_E$ with C_{NIPA} means that the degree of nonergodicity decreases with C_{NIPA}. This is accounted for by a dilution effect of cross-link density since R_{BIS} decreases with C_{NIPA} in the case of a fixed C_{BIS}.

Figure 9 shows C_{NIPA} dependence of $g_E^{(1)}(\tau)$ for (a) $R_{BIS} = 2.4$, (b) $R_{BIS} = 8.0$, and (c) 14.7 mol %. It is clear from these figures that $g_E^{(1)}(\infty) = 0$ for ergodic systems ($C_{NIPA} \le C_{NIPA}{}^{th}$) and $0 \ll g_E^{(1)}(\infty) < 1$ for nonergodic systems ($C_{NIPA} > C_{NIPA}{}^{th}$). The values of C_{NIPA} at which $g_E^{(1)}(\infty)$ becomes nonzero is in accordance with the $C_{NIPA}{}^{th}$ determined from the point at which a power-law behavior appears. Hence, it is concluded that the onset of gelation can be also determined by $g_E^{(1)}(\infty) \neq 0$.

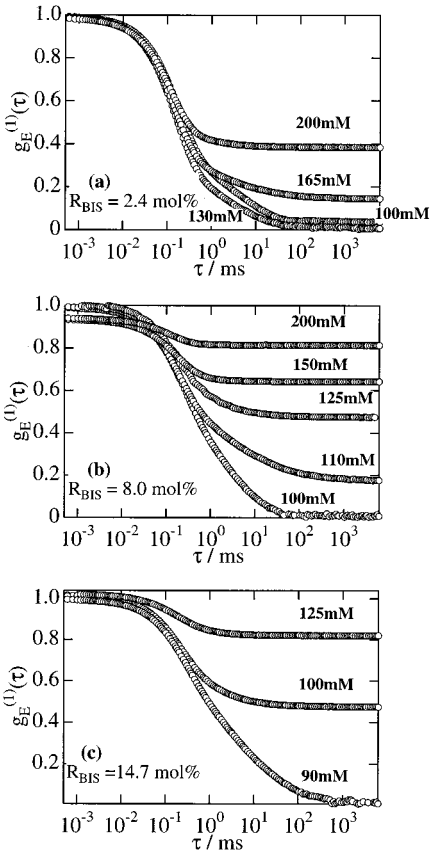

Figure 9. Variation of $g_E^{(1)}(\tau)$ with C_{NIPA} for (a) $R_{BIS} = 2.4$, (b) $R_{BIS} = 8.0$, and (c) 14.7 mol %.

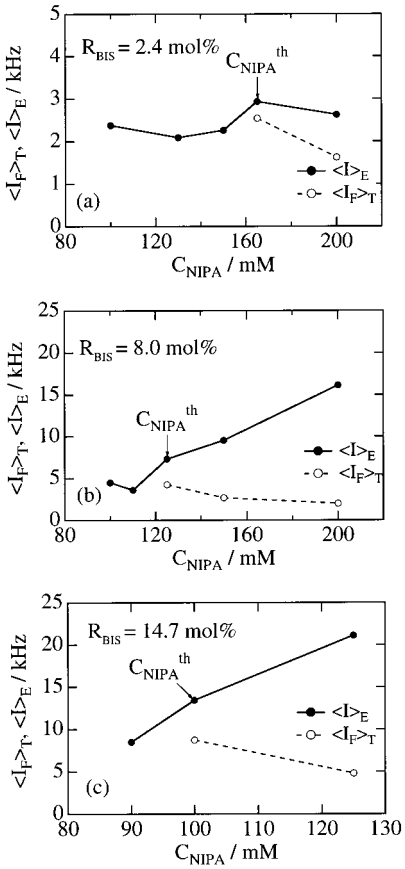

Figure 10. C_{NIPA} dependence of the scattered intensity component from thermal fluctuations, $\langle I_F\rangle_T$, and $\langle I\rangle_E$. C_{NIPA}^{th} indicates the NIPA concentration at which gelation takes place.

Figure 10 shows C_{NIPA} dependence of $\langle I\rangle_E$ and $\langle I_F\rangle_T$. Here, $\langle I\rangle_E$ seems to be an increasing function of C_{NIPA} except for the case of $R_{BIS} = 2.4$ mol %. Hence, unlike the case of a fixed C_{BIS}, one is tempted to conclude that $\langle I\rangle_E$ is an increasing function of C_{NIPA} for the case of fixed R_{BIS}. However, even in the case of a fixed C_{BIS}, a maximum in $\langle I\rangle_E$ appears around $C_{NIPA} \approx 200$ mM, which is beyond the range of the experiment. We presume that $\langle I\rangle_E$ has a maximum around C_{NIPA}^{th}. On the other hand, the decrease in $\langle I_F\rangle_T$ with increasing C_{NIPA} can be easily explained as suppression of thermal fluctuations of polymer chains due to a decrease of the mesh size with increasing C_{NIPA}.

Conclusion

The dynamics of cross-linked NIPA polymer chains with different monomer-cross-linker ratios, R_{BIS} (=2.4, 8.0, 14.7, and 22.0 mol %) was investigated by dynamic light scattering, and the following facts were disclosed: (1) The time−intensity correlation function (ICF) exhibited a power-law behavior exclusively at the gelation threshold. (2) A phase diagram for the sol−gel border, i.e., the locus of (C_{NIPA}^{th}, C_{BIS}^{th}) and the binodal line, was constructed, which is in good agreement with the site-bond percolation theory. The lower bound of C_{NIPA}^{th} is close to the so-called chain overlap concentration of monomer, C_{NIPA}*. (3) The dominant mode of the chain dynamics changes from collective diffusion to cluster diffusion at the gelation threshold. The relative strength of the collective mode is a function of R_{BIS}. (4) The power-law exponent in the time−intensity correlation function, n, was around 0.3 irrespective of R_{BIS}. (5) The C_{NIPA} dependence of the ensemble average scattered intensity, $\langle I\rangle_E$, was different between the case with constant C_{NIPA} and the case with constant R_{BIS}. All of these facts were successfully interpreted with a physical picture of cross-linked polymer chain clusters.

Acknowledgment. This work is partially supported by the Ministry of Education, Science, Sports and Culture, Japan (Grant-in-Aid, 09450362, 10875199, and 11305067). Thanks are due to the Cosmetology Research Foundation, Tokyo, for financial assistance. T.N. acknowledges the Research Fellowship of the Japan Society for the Promotion of Science for Young Scientists.

References and Notes

(1) For example: Brown, W. *Dynamic Light Scattering, the Methods and Applications*; Clarendon Press: Oxford, 1993.
(2) Martin, J. E.; Wilcoxon, J.; Adolf, D. *Phys. Rev. A* **1987**, *36*, 1803.
(3) Martin, J. E.; Wilcoxon, J. *Phys. Rev. Lett.* **1988**, *61*, 373.
(4) Martin, J. E.; Wilcoxon, J.; Odinek, J. *Phys. Rev. A* **1991**, *43*, 858.
(5) Lang, P.; Burchard, W. *Macromolecules* **1991**, *24*, 814.
(6) Ren, S. Z.; Shi, W. F.; Zhang, W. B.; Sorensen, C. M. *Phys. Rev. A* **1992**, *45*, 2416.
(7) Adam, M.; Lairez, D. *Sol-Gel Transition*; Cohen Addad, J. P., Ed.; John Wiley & Sons: New York, 1996; p 87.
(8) Norisuye, T.; Takeda, M.; Shibayama, M. *Macromolecules* **1998**, *31*, 5316.
(9) Norisuye, T.; Shibayama, M.; Tamaki, R.; Chujo, Y. *Macromolecules* **1999**, *32*, 1528.
(10) Tanaka, T.; Hocker, L. O.; Benedek, G. B. *J. Chem. Phys.* **1973**, *59*, 5151.
(11) Ikkai, F.; Shibayama, M. *Phys. Rev. Lett.* **1999**, *82*, 4946.
(12) Coniglio, A.; Stanley, H. E. *Phys. Rev. Lett.* **1979**, *42*, 518.
(13) Pusey, P. N.; van Megen, W. *Physica A* **1989**, *157*, 705.

(14) Joosten, J. G. H.; McCarthy, J. L.; Pusey, P. N. *Macromolecules* **1991**, *24*, 6690.
(15) Winter, H. H.; Chambon, F. *J. Rheol.* **1986**, *30*, 367.
(16) Doi, M.; Onuki, A. *J. Phys. II* **1992**, *2*, 1631.
(17) Muthukumar, M. *Macromolecules* **1989**, *22*, 4656.
(18) Muthukumar, M.; Winter, H. H. *Macromolecules* **1986**, *19*, 1284.
(19) Norisuye, T.; Shibayama, M.; Nomura, S. *Polymer* **1998**, *39*, 2769.
(20) Shibayama, M.; Isaka, Y.; Shiwa, Y. *Macromolecules* **1999**, *32*, 7086.
(21) Shibayama, M.; Fujikawa, Y.; Nomura, S. *Macromolecules* **1996**, *29*, 6535.
(22) Onuki, A. *J. Non-Cryst. Solids* **1994**, *172*−*174*, 1151.
(23) Muthukumar, M. *J. Chem. Phys.* **1985**, *83*, 3161.
(24) Martin, J. E.; Adolf, D.; Wilcoxon, J. P. *Phys. Rev. A* **1989**, *39*, 1325.
(25) Antonietti, M.; Foelsch, K. J.; Sillescu, H.; Pakula, T. *Macromolecules* **1989**, *22*, 2812.

MA9921044